PHILOSOPHICAL MAGAZINE, 2003, VOL. 83, NO. 10, 1191–1204

# Undissociated screw dislocations in silicon: calculations of core structure and energy

L. PIZZAGALLI†, P. BEAUCHAMP and J. RABIER

Laboratoire de Métallurgie Physique, Unité Mixte de Recherche 6630 du CNRS, Université de Poitiers, BP 30179, 86962 Futuroscope Chasseneuil Cedex, France

[*Received 27 August 2002 and accepted in revised form 27 November 2002*]

ABSTRACT

The stability of the perfect screw dislocation in silicon has been investigated using both classical potentials and first-principles calculations. Although a recent study by Koizumi *et al.* stated that the stable screw dislocation was located in both the 'shuffle' and the 'glide' sets of {111} planes, it is shown that this result depends on the classical potential used, and that the most stable configuration belongs to the 'shuffle' set only, in the centre of one $(\bar{1}01)$ hexagon. We also investigated the stability of an $sp^2$ hybridization in the core of the dislocation, obtained for one metastable configuration in the 'glide' set. The core structures are characterized in several ways, with a description of the three-dimensional structure, differential displacement maps and derivatives of the disregistry.

## § 1. INTRODUCTION

Dislocations in silicon have been the subject of many investigations, experimental, computational and theoretical, not only because they can appear in microelectronic devices, but also because of their own properties, closely related to the covalent nature of bonding in this material. In ordinary conditions, silicon is brittle below about 600°C (Hirsch, Samuels and Roberts 1989, George and Michot 1993). Above this temperature, transmission electron microscopy observations show dissociated dislocations (Ray and Cockayne 1971) which thus lie between the narrowly spaced {111} planes, that is belonging to the glide set. On the basis of computed generalized stacking-fault energy and entropy calculations on {111} narrowly spaced (glide set) and widely spaced (shuffle set) respectively (Kaxiras and Duesbery 1993), the idea was put forward of the possibility of a transition; at low temperatures, perfect dislocations are easier to nucleate and move in the shuffle set, while the activation barrier for glide becomes lower for dissociated dislocations in the glide set at high temperatures (Duesbery and Joos 1996).

Thus, experiments have been undertaken in which, in order to achieve plastic deformation at temperatures as low as room temperature, the silicon sample is either submitted to a high confining pressure, of the order of 5 GPa (Rabier *et al.* 2001), or subjected to a surface scratch test (Rabier *et al.* 2000). Under these conditions, the microstructure has been found to be formed of undissociated dislocations, supposed to belong to the shuffle set. Favoured dislocation orientations appear to be screw,

† Email: Laurent.Pizzagalli@univ-poitiers.fr.

*Philosophical Magazine* ISSN 1478–6435 print/ISSN 1478–6443 online © 2003 Taylor & Francis Ltd
http://www.tandf.co.uk/journals
DOI: 10.1080/0141861031000071999

60°, 30° and also 41°. Similarly, deformation experiments in III–V compounds such as GaAs, InP and InSb, performed at temperatures down to 77 K by applying a high confining pressure (Suzuki *et al.* 1998, 1999a, b), indicate that the low-temperature plastic deformation is governed by kink pair formation on undissociated screw dislocations moving in the shuffle set planes.

Theoretical investigations of the core structures of dislocations in silicon are then clearly required to bring additional insights. However, despite a large number of existing atomistic computations, most of these were devoted to partial dislocations of the glide set, with a particular attention to core reconstructions of the 30° and 90° partials and to mobility properties (cf. for instance the review by Bulatov *et al.* (2001)). Less information is available about perfect dislocations. In his pioneering examination of dislocation cores in diamond cubic structures, Hornstra (1958) quite naturally placed the screw dislocation line furthest away from any atom row, that is at the centre of the hexagon formed by six neighbouring $\langle 110 \rangle$ dense atom rows; the dislocation then belongs to the shuffle set; more precisely it is located at the intersection of two $\{111\}$ shuffle planes at 71.53°. By somewhat artificially rebonding atoms, Hornstra also proposed another structure for the screw core, the interesting idea being that the core is spread over two adjacent hexagons sharing a common small edge. Arias and Joannopoulos (1994) performed density functional theory (DFT) calculations of the shuffle screw dislocation in silicon; they found the first configuration proposed by Hornstra to be stable with respect to spontaneous dissociation and they calculated energy parameters for the core. Finally, in a recent study, Koizumi *et al.* (2000) have investigated the core configuration and the mobility of the $(a/2)\langle 110 \rangle$ screw dislocation using the Stillinger–Weber (SW) (1985) potential for silicon. They found two stable configurations: the configuration at the centre of the hexagon, denoted A, has a higher energy and the lower-energy configuration (denoted B) can be regarded as belonging to both a $\{111\}$ shuffle plane and the $\{111\}$ glide plane at 71.53°. Koizumi *et al.* discussed in detail the very special part that configuration B might play in the cross-slip mechanism and in the transition of dislocation glide from the shuffle set to the glide set. It remains to be confirmed whether these results are general and not specific to the SW potential. Regarding the glide set, previous work essentially focused on partial dislocations, and, to our knowledge, there are no available studies of the perfect screw configurations.

Thus, it is of interest to investigate the core properties of perfect dislocations in the shuffle and glide sets, and in particular the existence and relative stability of all proposed configurations of the screw orientation. This paper reports such calculations, using both DFT formalism and several semiempirical potentials. After a description of the methods and computational details, we present the different energy and structural parameters associated with each configuration. These quantities are then discussed in relation with the previous results, dislocation mobilities and validity of the classical potentials.

## § 2. Computational methods

The atomistic calculations have first been carried out using semiempirical potentials. We have employed the following potentials:

(i) the SW potential, used as reference and also for comparison with previous work from Koizumi *et al.* (2000);

(ii) the Tersoff (1988) potential which is able to give a better representation of a number of defects than the SW potential does;
(iii) the EDIP (Justo *et al*. 1998) constructed so as to benefit from the successes of earlier potentials and incorporating data obtained from DFT calculations, such as the $\gamma$ surfaces.

It has to be noted that, for dislocation calculations, the EDIP is the only semiempirical potential able to account for reconstructions of both 30° and 90° partials in the glide set. The main advantage of empirical potentials is their low computational cost, which allows fast calculation of several configurations. Potentials suffer from limitations, implicitly related to their functional form or limited fitting database, and calculated energies may prove to be relatively inaccurate, especially for configurations involving highly distorted or broken bonds, as encountered in dislocation cores. However, by using three different types of potential, we expect to overcome this issue and to obtain reliable results.

First-principles calculations have also been carried out, in order to discriminate between configurations, and to calculate more precise defect energies. In addition, comparisons with empirical potential allowed us to check their reliability for dislocation core investigations. We performed DFT calculations (Hohenberg and Kohn 1964, Kohn and Sham 1965) in the local density approximation at zero temperature with the ABINIT (2002) code†. The ionic interactions were represented by norm-conserving pseudopotentials (Trouiller and Martins 1991). We used a plane-wave basis with an energy cut-off of 10 Ry and two special $k$ points along the dislocation line (Monkhorst and Pack 1976). Tests with the generalized gradient approximations (GGAs), a higher-energy cut-off or a finer $k$-point sampling have also been conducted for selected configurations. We found an error on the defect energy lower than 0.5% using five special $k$ points and a cut-off of 14 Ry, and about 5% when using GGAs.

At first, semiempirical potential calculations were made, for a fast exploration of several system sizes, thus determining the size effects of the simulation slab on the results. Suitable simulation box sizes were then selected, small enough for DFT calculations to remain tractable and large enough for the computed energies to be meaningful.

## § 3. Simulation model

Ideally, we would consider an isolated straight screw dislocation in an infinite bulk. Along the dislocation line, provided that there is no reconstruction, we have a periodic situation with a period equal to the Burgers vector $a_0\frac{1}{2}[110]$. Periodic boundary conditions are then the most suitable choice along the dislocation line. In the plane perpendicular to the dislocation line, a long-range strain field will be generated by the dislocation and should be taken into account in the calculation. Two different methods could be employed.

In the first, no periodic boundary conditions perpendicular to the dislocation line are applied, and only one dislocation is located in the centre of the simulation box (figure 1, configuration A). The atomic positions at the boundaries are then initialized to values calculated with elasticity theory using a numerical code adapted

† The ABINIT code is a common project of the Université Catholique de Lourain, Corning Incorporated and other contributors.

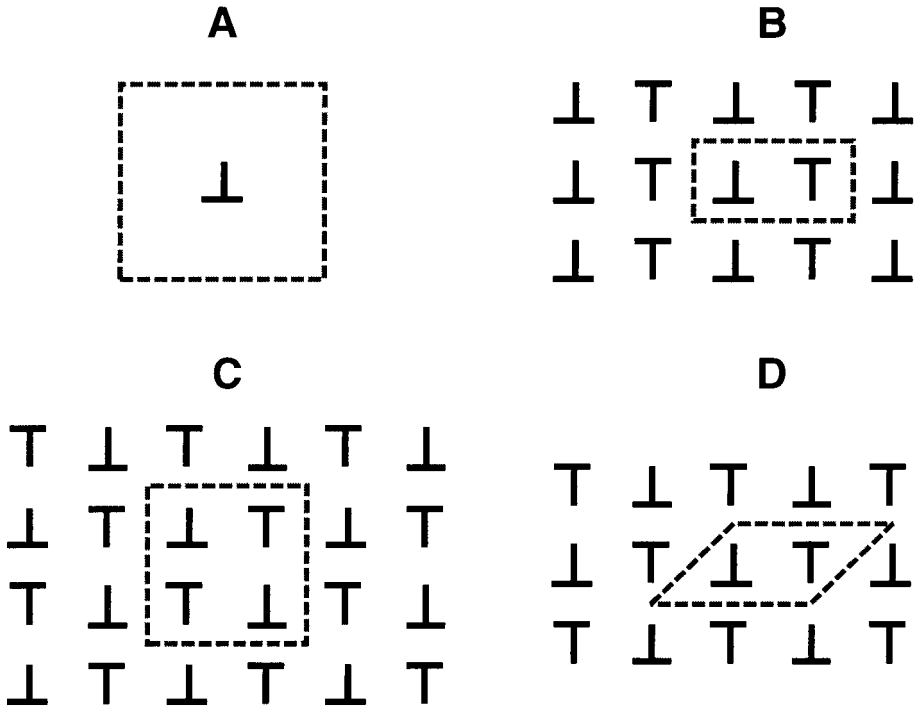


Figure 1. Models for straight dislocation simulations. For A, there is no periodic boundary conditions and only one dislocation in the computational cell (broken lines). B, C and D show periodic boundary systems with dipolar (B) or quadrupolar (C, D) distributions of dislocations.

from ANCALC (Stroh 1958, 1962) or with a more precise model (Lehto and Öberg 1998). The computational box has to be large enough to prevent a fictitious interaction between fixed boundaries and the dislocation core. In addition, atoms located at the edges of the system are not in a bulk-like environment, and defect energies can not be directly extracted from total energy calculations. Here, we used such an approach for semiempirical potential calculations only, because the simulation box could be enlarged at will, owing to the low computational cost, and also because defined individual atomic energy allows an easy determination of defect energies. Typical computational cells involved about 10 000 atoms (dimensions $133\,\text{Å} \times 132\,\text{Å} \times 11.5\,\text{Å}$ for a $40 \times 84 \times 3$ cell). The anisotropic elastic energy per unit length of the dislocation is given by the well-known formula (Hirth and Lothe 1982)

$$E = \frac{K\mathbf{b}^2}{4\pi} \ln\left(\frac{R}{r_0}\right).$$

The second method involves periodic boundary conditions along the directions perpendicular to the dislocation line. In that case, annoying difficulties arise owing to discontinuities at the boundaries, in particular for a single dislocation. Spurious shear strain associated with these discontinuities could then have a significant influence on the dislocation core structure and energetics. These difficulties can be smoothed by considering dipolar (figure 1, configuration B) or quadrupolar (figure 1,

configuration C) arrangements of dislocations in the cell. Whether a dipole or a quadrupole should be favoured depends on the character of the dislocation; a dipole is best suited to an edge dislocation whereas a quadrupole minimizes the residual strain associated with a quadrupole of screw dislocations (Lehto and Öberg 1998). With the second choice, four dislocations should be included in the cell, with separation distances large enough to prevent a spurious interaction, which would lead to large cell sizes. However, as suggested by Bigger *et al.* (1992), the system could be divided by a factor of two by relaxing the orthogonality constraints on the periodic cell (figure 1, configuration D). In this work, the quadrupolar arrangements of dislocations (figure 1, configurations C and D) have been considered for both semiempirical and first-principles calculations. The semiempirical calculations were useful for investigating easily several cell sizes and estimating the non-elastic core–core energy contributions possibly present for very small cells. We considered computational cells ranging from $40 \times 84 \times 3$ to $6 \times 12 \times 3$. For *ab initio* calculations, the largest $12 \times 12 \times 1$ cell encompasses 144 atoms, with two dislocations.

For a quadrupolar distribution and four dislocations in an orthogonal cell, the anisotropic elastic energy per unit length is obtained by summation of the interactions between dislocation pairs, calculated using a code adapted from ANCALC (Stroh 1958, 1962). The total energy can be split up into an interaction energy inside the cell ($E^{\text{intra}}$) and half the interaction energy between the quadrupole and all its periodically repeated images ($E^{\text{inter}}$). A reference (zero) of the elastic energy is required for determining $E^{\text{intra}}$ and is chosen as the elastic energy of a dislocation's quadrupole whose distance along the edge is $d_0$. In that case, it can be shown that the reference distance $d_0$ is equal to the core radius $r_0$ obtained for a single dislocation. In fact, if the quadrupole is extremely large such that the four dislocations can be considered as isolated, the elastic energy amounts to four times the self energy of a single dislocation. The determination of $E^{\text{inter}}$ should require an infinite summation but, in practice, the convergence is quickly achieved. It has to be noted that this is not the case for a dipolar arrangement, and special handling of the summation is required (Cai *et al.* 2001). The derivation of the elastic energy for a quadrupolar distribution in a non-orthogonal cell (two dislocations per cell instead of four; see figure 1) is straightforward.

## § 4. Results

Table 1 shows the elastic constants calculated with the semiempirical potentials and first principles. These constants are used for generating the initial configurations from anisotropic elasticity theory, and extracting core energetics from relaxed systems.

In figure 2, we show a $(\bar{1}01)$ section of the cubic diamond structure, with three possible locations of the dislocation line. A corresponds to the original position at the centre of one hexagon (Hornstra 1958), for a screw dislocation belonging to two shuffle planes. B was recently proposed by Koizumi *et al.* (2000), at the middle of one long hexagon bond. It is interesting to point out that, in this case, the dislocation is located at the crossing of both a shuffle and a glide $\{111\}$ plane. Finally, another high-symmetry location on the structure occurs at C, at the middle of a short hexagon bond, with the screw dislocation belonging to two glide planes. Other locations have been investigated, either inside the hexagon or at the exact position of one silicon atom but, in all cases, the system relaxed to one of the three selected configurations.

Table 1. Experimental (Simmons and Wang 1971) and calculated elastic constants for the SW (1985) potential, Tersoff (1989) potential and the EDIP (Justo *et al.* 1998) as well as our *ab initio* results. The SW parameters have been rescaled in order to fit the experimental cohesive energy of 4.63 eV. For a screw dislocation in a cubic diamond structure, $K = [C_{44}(C_{11} - C_{12})/2]^{-1/2}$.

| | Experimental value | Value calculated using the following methods | | | |
|---|---|---|---|---|---|
| | | SW potential | Tersoff potential | EDIP | *Ab initio data* |
| $B$ (Mbar) | 0.99 | 1.083 | 0.978 | 0.99 | 0.99 |
| $C_{11}$ (Mbar) | 1.67 | 1.617 | 1.425 | 1.75 | 1.64 |
| $C_{12}$ (Mbar) | 0.65 | 0.816 | 0.754 | 0.62 | 0.66 |
| $C_{44}$ (Mbar) | 0.81 | 0.603 | 0.687 | 0.71 | 0.78 |
| $C_{44}^0$ (Mbar) | | 1.172 | 1.188 | 1.12 | 1.09 |
| $K$ | 0.64 | 0.49 | 0.48 | 0.63 | 0.62 |

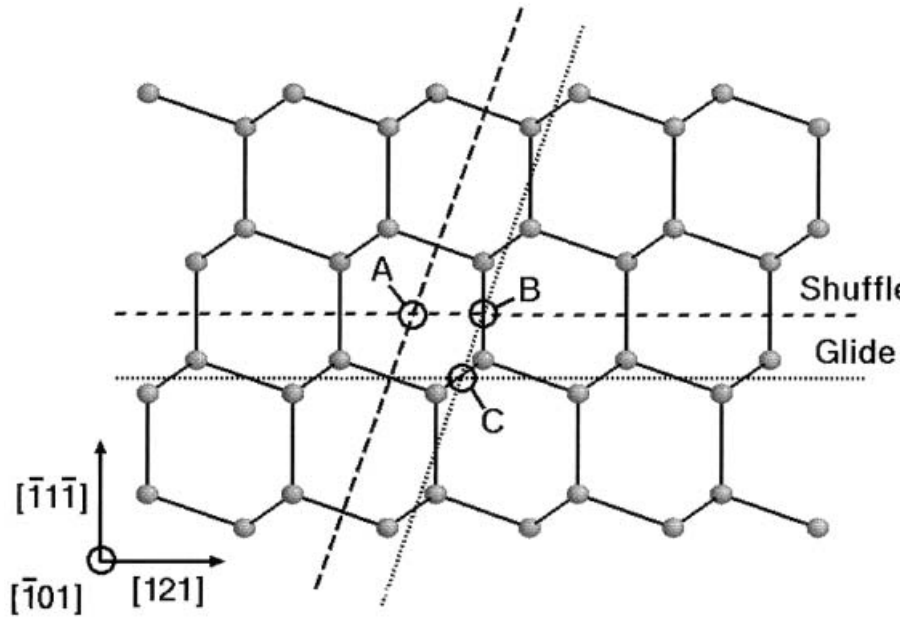


Figure 2. Ball-and-stick representation of the ($\bar{1}01$) plane of the cubic diamond structure. The three circles A, B and C indicate the positions of the dislocation line. Broken (dotted) lines show the 'shuffle' ('glide') {111} planes.

The different energy values resulting from all our calculations are reported in table 2. The energy differences show that, with *ab initio* and all potentials but SW, configuration A is the most stable. We were able to reproduce the results of Koizumi *et al.* (2001), B appearing more stable than A by using the SW potential. B is obtained as the second choice with the *ab initio* potential and the EDIP, while it seems highly unfavourable with the Tersoff potential. Another important point concerns the stability of configuration B. Although the relaxation with semiempirical potentials was straightforward, the geometry of B has been found to be extremely difficult to retain within a first-principles calculation, even using initial configura-

Table 2. Calculated energy parameters for A, B and C screw dislocations. $\Delta E$ is the energy difference with an uncertainty of 0.01 eV per Burgers vector. $r_0$ is the core radius ($\pm 0.03$ Å). $E_c$ is the core energy, obtained with a fixed core radius equal to the Burgers vector ($\pm 0.02$ eV Å$^{-1}$). Note that C is not stable with the SW potential; it relaxed to a configuration with an energy 0.02 eV per Burgers vector higher than A.

| | $\Delta E$ (eV per Burgers vector) | | Radius $r_0$ (Å) | | | Energy $E_c$ (eV Å$^{-1}$) | | |
|---|---|---|---|---|---|---|---|---|
| | $E_B - E_A$ | $E_C - E_A$ | A | B | C | A | B | C |
| SW | −0.14 | | 0.82 | 0.91 | | 0.55 | 0.51 | |
| Tersoff | 1.08 | 0.54 | 0.78 | 0.35 | 0.52 | 0.55 | 0.84 | 0.70 |
| EDIP | 0.23 | 0.74 | 1.49 | 1.32 | 0.98 | 0.37 | 0.42 | 0.54 |
| *Ab initio* | 0.32 | 0.86 | 1.22 | 1.03 | 0.74 | 0.52 | 0.60 | 0.74 |

tions relaxed with potentials as a starting point. Some or all dislocations of the quadrupole generally evolved to configuration A or annihilated themselves. Only in one case were we able to relax the structure. Finally, for all calculations, configuration C is never the most stable or is even unstable with the SW potential.

Table 2 also reports the core radii obtained by matching the elastic energy with the calculated defect energy. For the empirical potential calculations and one unique dislocation in the computational cell, the core radius $r_0$ is determined by considering the defect energy contained in the cylinder centred on the dislocation line, with radius $R$ and height equal to the Burgers vector **b** (see formula above). The factor $K$ determined from the calculated elastic constants is used. We considered that the core radius $r_0$ is already well converged for $R = 60$ Å. For example, the core radius changes by less than 0.01 Å for $R$ ranging between 40 and 60 Å, for configuration A and the SW potential. For first-principles calculations and a quadrupolar distribution of dislocations, the core radius is determined numerically by inverting the defect elastic energy. We found that the core radius determination is already very precise for a $12 \times 12$ cell, with an uncertainty about 0.01 Å. For the smaller $6 \times 6$ cell, a 0.1 Å deviation from converged values was obtained. Most of the values are close to about 1 Å, the commonly used value that is a quarter of the Burgers vector. Only core radii for B and C with the Tersoff potential and for A with the EDIP are slightly distant. In table 2, core energy values, often used in the literature, which are obtained with a core radius equal to the Burgers vector, are also reported.

Figure 3 shows differential displacement maps of the relaxed configurations A, B and C of the screw dislocations, obtained from systems with one unique dislocation and relaxed with an empirical potential. For configuration A, the distortion is uniformly distributed on the hexagon ring encircling the dislocation line. It is also clear from the figure that the displacements are identical along the two 'shuffle' planes (see figure 2). Configuration B is characterized by a maximal distortion on the two atoms on both sides of the 'shuffle' plane. Most of the constraints are located on the hexagon rings sharing these atoms. In the case of configuration C, the maximal distortion is also located on two atoms, but on both sides of a 'glide' plane. Average deformations are observed for all four hexagon rings around these two atoms, and equivalent displacements along the two glide planes passing through the C screw dislocation core. It is noteworthy that, for each geometry, almost identical pictures have been obtained regardless of the potential considered. One exception is configuration C with the SW potential, which relaxes to configuration C represented in figure 3. The initial differential displacement located on the two

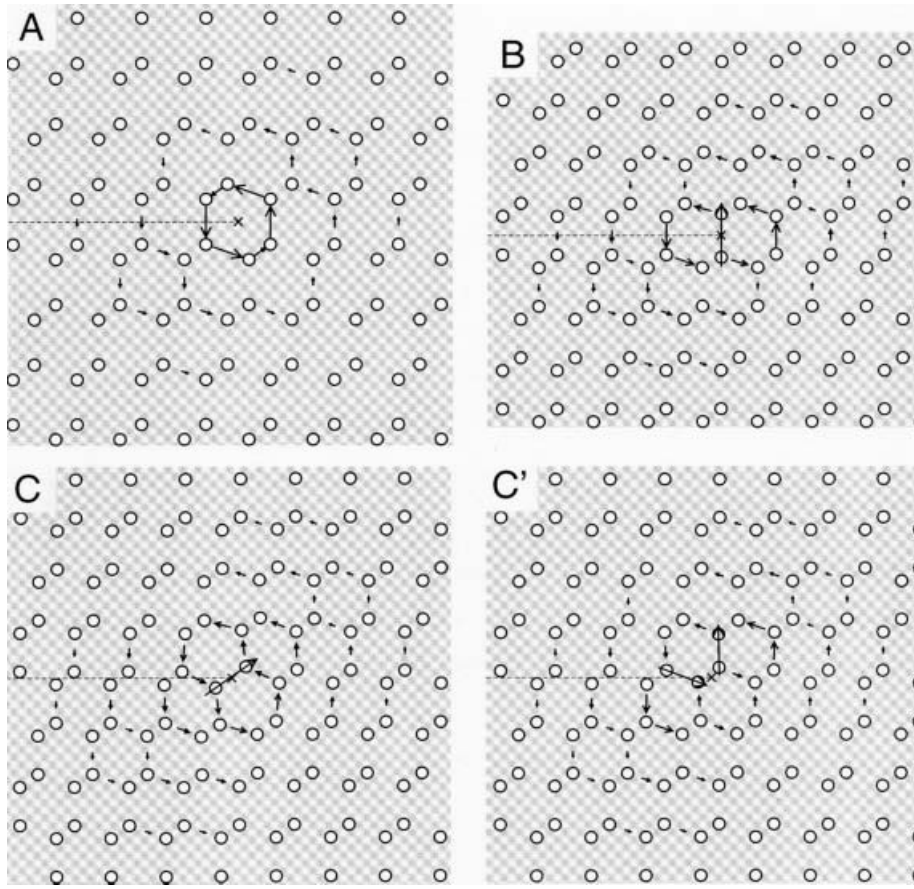


Figure 3. Differential displacement maps of the screw dislocation in configurations A, B, C and C′ (obtained with SW from C). The arrows are proportional to the out-of-plane $[\bar{1}01]$ shifts between neighbouring atoms introduced by the dislocation. The cross indicates the position of the dislocation line and the broken line the cut plane.

atoms next to the dislocation location vanished, and large distortions appeared involving more distant atoms (see figure 3). We found this configuration to be unstable with both the EDIP and the Tersoff potential, relaxing to A. In figure 4, the differential displacement map for a quadrupolar distribution of configuration A, relaxed with first principles, is represented. Even if the dislocation cores are close and interact together, it is noteworthy that the general pattern obtained for a unique dislocation remains easily recognizable in that case.

To characterize the spatial extension of the dislocation core, we have determined the width at half-maximum (WHM) of the derivative of the disregistry introduced by the dislocation. The disregistry is obtained by computing the difference of displacements along $(\bar{1}01)$ for atoms on either sides of the glide $(\bar{1}1\bar{1})$ plane (figure 5). The calculated points are fitted on the simple shape $\arctan(x/\Delta)$ of a dislocation (Hirth and Lothe 1982). The determination of the WHM is then straightforward. In table 3, we report all values, as well as the WHM calculated in the same way for configurations built from anisotropic elasticity theory. In contrast with the energy ordering, it appears that the WHMs do not depend on the kind of classical potential, for a given

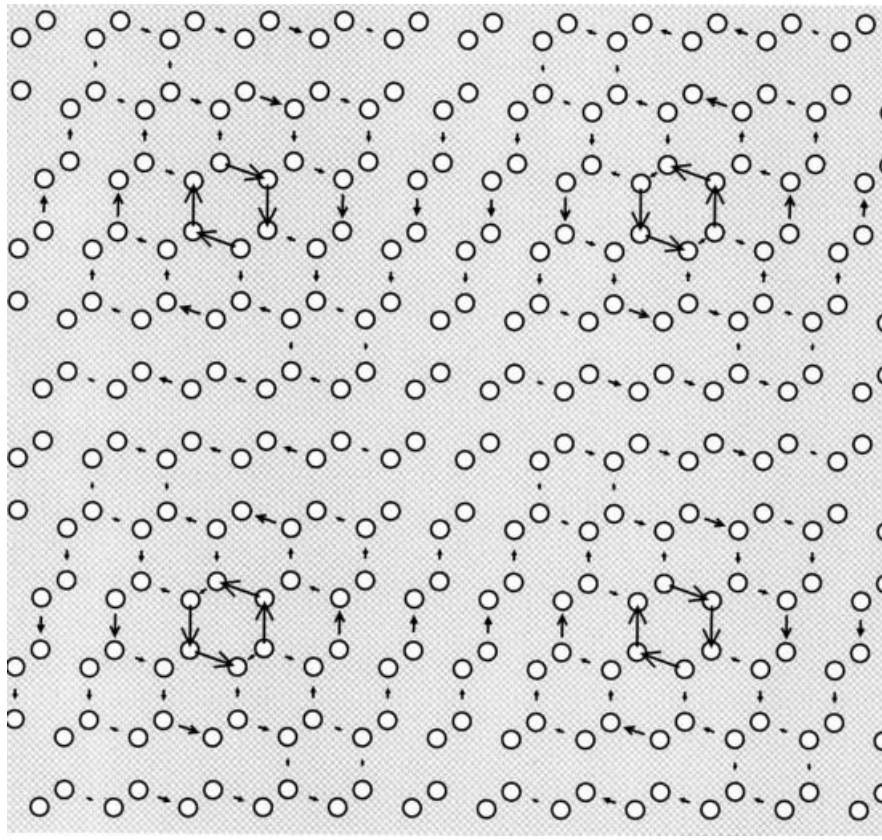

Figure 4. Differential displacement maps of the screw dislocation in configuration A, in the quadrupolar distribution shown in the figure 1. The arrows are proportional to the out-of-plane $[\bar{1}01]$ shifts between neighbouring atoms introduced by the dislocation.

configuration. For C, the *ab initio* WHM is also equal to the classical value. It is also clear that the B core is wider than the A core.

## § 5. Discussion

Configuration A has been considered as the most plausible structure for the undissociated screw dislocation in silicon, but a recent study by Koizumi *et al.* (2000) concluded that configuration B is slightly more stable than configuration A. Our calculations indicate that A is definitely the most stable geometry for the screw dislocation, using *ab initio* and two classical potentials. However, with the SW potential, we were able to reproduce the result of Koizumi *et al.*, which proves that the apparent stability of B over A is an artefact of the potential. With first-principles calculations involving various cell sizes, configuration B was found to be stable in only one case. It seems that the slightest deformation could lead to the relaxation from B to A. We conclude that configuration B is weakly metastable. Additional insights are obtained from the analysis of the core. Figure 6 shows three-dimensional structures of three configurations. A is characterized by the absence of atomic rearrangements in the core, the main distortions being located on all bonds forming the hexagon ring encircling the dislocation core. On the contrary, for B, the

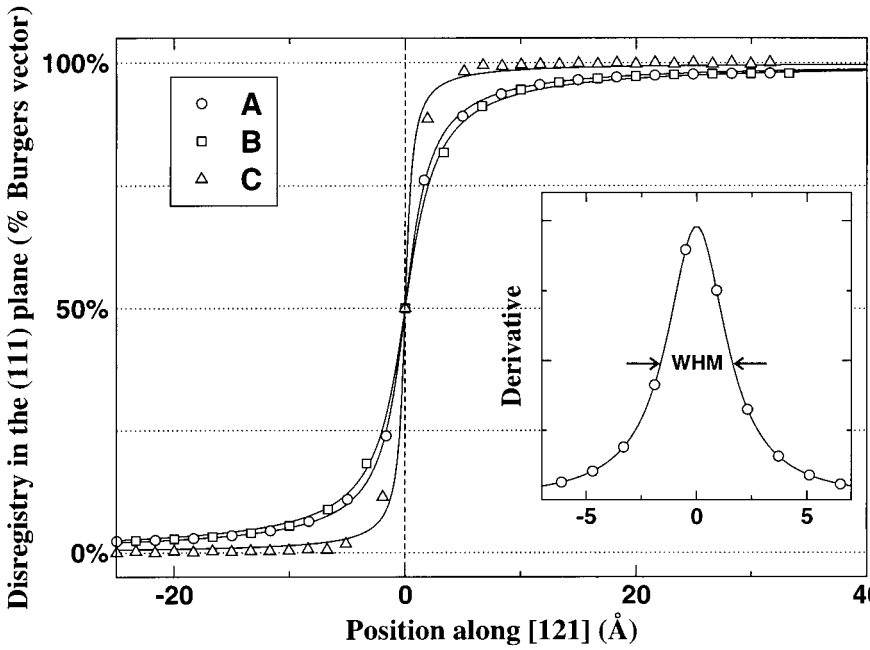


Figure 5. Variation in the disregistry in the (111) plane along the [121] direction for the three configurations. The solid curves are fits with the expression $f(x) = b[(1/\pi)\arctan(x/\Delta) - \frac{1}{2}]$. The inset graph shows the derivative of the disregistry for A, and the definition of the WHM.

Table 3. WHM obtained from elasticity (with experimental $C_{ij}$), classical potentials and *ab initio* data. Two values are undetermined, owing to the instability of C with SW, and the difficulty in obtaining B from first principles in a large cell.

| | WHM (Å) obtained using the following methods | | | | |
|---|---|---|---|---|---|
| | Elastic | SW potential | Tersoff potential | EDIP | *Ab initio* |
| A | 2.7 | 3.1 | 3.2 | 3.2 | 3.6 |
| B | 2.6 | 3.9 | 4.0 | 4.0 | |
| C | 1.2 | | 0.9 | 0.9 | 0.9 |

main deformations are located on the two atoms close to the core. They are bonded together and at the same height along $(\bar{1}01)$ in the bulk. After introduction of the dislocation, the atoms now have a height difference of half the Burgers vector along $(\bar{1}01)$, and they are separated by about 2.8 Å. Weak bonds with such an interatomic distance are possible for silicon. However, each of these atoms already has a coordination of 3 and would need to accommodate two extra bonds (see figure 6), which is unlikely to occur. From the analysis of the electronic density, it appears that, in the core of B, two rows of dangling bonds follow the dislocation line. On the one hand, these rows may explain the very low stability of this configuration with first-principles methods. On the other hand, the large range of energy values illustrates the difficulty of describing dangling bonds with the classical potentials. The WHM and therefore the core extension of B are larger than those of A, which may also explain why B is less stable.

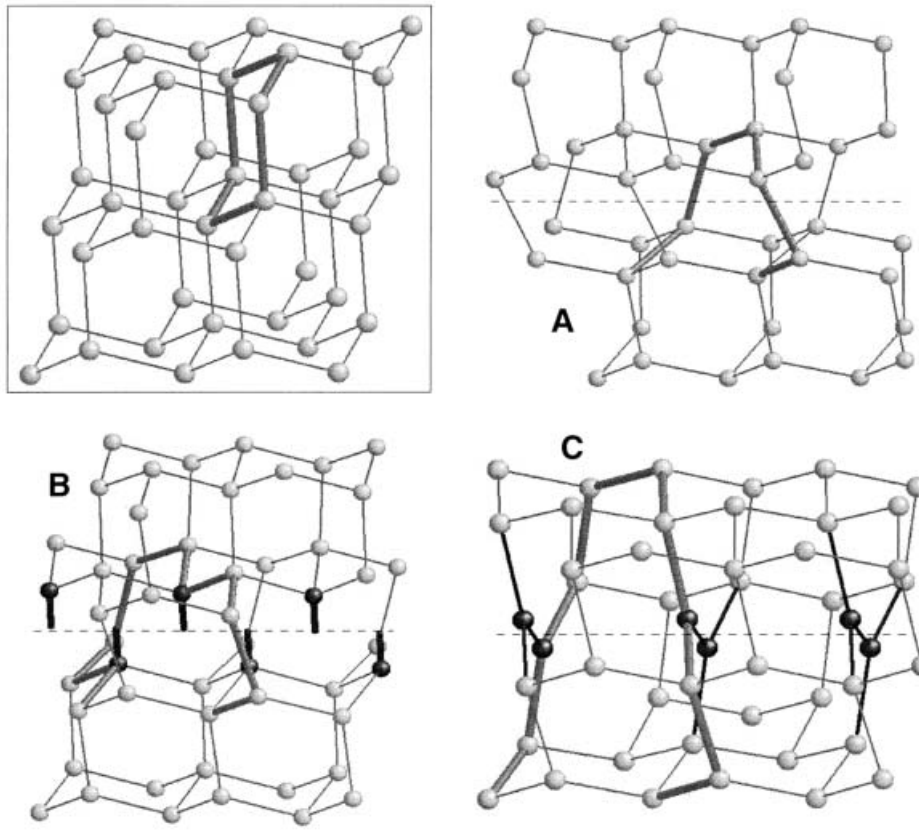


Figure 6. Ball-and-stick representation of the cubic diamond bulk (top left) and of the three screw core configurations. A six-atom ring (see figure 2) is represented by dark grey sticks, in order to show the deformation due to the dislocation and the Burgers vector. Dangling bonds (for B) and $sp^2$ atoms (for C) are represented by black sticks and balls. The position of the dislocation line is shown by the broken lines.

We also investigated the possibility of a screw dislocation in the glide set with configuration C. With all classical potentials and the first-principles method, it is found that A is more stable than C, with a large energy difference. It is then unlikely that the core of C could be formed in bulk silicon. However, interesting features are associated with this structure. The examination of the geometry in the core revealed that the two atoms on either side of the dislocation line (dark balls in the ball-and-stick representation in figure 6) have a coordination of 3. Before the introduction of the dislocation, these two atoms were bonded together, with a height difference of half the Burgers vector along $(\bar{1}01)$. After the introduction of the dislocation, they are still bonded together but located at the same height, one bond per atom being broken. The *ab initio* interatomic distance between these two atoms is 2.16 Å, whereas distances from neighbouring atoms are about 2.29 Å. The three bonds for each atom are almost coplanar, and the angle between them ranged from 117° to 123°. All these quantities indicate an $sp^2$ hybridization of these two atoms, with a double bond between them, which is confirmed by the analysis of the electronic density. This possibility has already been proposed by Hornstra (1958), on the

basis of geometrical arguments only. An $sp^2$ hybridization is not favoured in silicon, which explained the large defect energy for configuration C. However, it would be interesting to investigate the competition between screw configurations in diamond for example, where $sp^2$ is favoured over $sp^3$. It is worth noting that an $sp^2$ character is also present in recently proposed metastable structures for the 30° and 90° partial dislocations in diamond (Ewels *et al.* 2001, Blumenau *et al.* 2002). One interesting aspect of configuration C is the tightness of the core. It is difficult to compare A and C directly since they are not located in the same family of 111 planes. Nevertheless, insights could be gained by the comparison with the anisotropic elastic solution (table 3). It is clear that for all potentials, and especially for the *ab initio* potential, the relaxed A core is wider than the initial elastic configuration. The effect is even stronger for configuration B. However, in the case of C, the core is contracted by the atomic relaxation. The narrowness of C could be partly attributed to the formation of the double bond in the core.

To our knowledge, configuration A has already been investigated with first-principles techniques in two previous studies. Arias and Joannopoulos (1994) found a core energy $E_c = 0.56 \pm 0.21$ eV Å$^{-1}$ whereas Miyata and Fujiwara (2001) obtained $E_c$ equal to 0.95 eV Å$^{-1}$. These results may be compared with our *ab initio* core energy of 0.52 eV Å$^{-1}$ (table 2), very close to the value of the former study. However, this agreement seems fortuitous, as Arias and Joannopoulos used isotropic theory and a fitted $K \equiv \mu = 0.29$ eV Å$^{-3}$. Miyata and Fujiwara (2001) followed a similar approach, but with a fitted $K \equiv \mu = 0.48$ eV Å$^{-3}$ and obtained a larger core energy. Instead, here, $K$ factors calculated within anisotropic theory and with the *ab initio* calculated elastic constants, very close to the experimental values (see table 2), are employed. The disagreement between the different studies may be explained by the poor $k$-point sampling in the newer study, as well as the use of isotropic theory with a fitted $K$ factor.

We discussed our results in relation to the screw mobility. As configuration A has the most stable geometry, possible paths from one minimum to another include saddle configurations B or C (see figure 2). Koizumi *et al.* (2000) found a Peierls stress of about 2 GPa for the non-dissociated screw dislocation, considering the path A → B → A. However, this relatively low value may be explained by the use of the SW potential, and its failure to yield the correct stability of configurations A and B. In fact, although the Peierls stress cannot be simply determined from static calculations, several insights may be obtained from the analysis of the energy differences between configurations. With SW, the energy difference between A and B is only 0.14 eV per Burgers vector. With first principles, we determined a larger energy difference of 0.32 eV per Burgers vector. It is then reasonable to assume that the Peierls stress for the path A → B → A will be much higher than 2 GPa. This is confirmed by recent *ab initio* calculations by Miyata and Fujiwara (2001), where the Peierls stress ranged from 22 to 30 GPa. Another possible path for dislocation cross slip would be A → C → A. However, the large calculated energy difference indicates a very large stress, and this possibility may be ruled out solely on the basis of energy considerations.

Finally, we compared the merits of the classical potentials that we have used in this study. On the basis of our three investigated configurations, it appears that the EDIP is more suitable than the SW or the Tersoff potential for this study, the stability and energy differences being close to the *ab initio* results. This is not completely surprising since this potential has been designed specifically to study defects

(Justo *et al*. 1998). The worst is maybe the SW potential, which yields the B core as the most stable configuration. It is worth noting that, although the stabilities of the different core configurations very much depend on the kind of potential, we obtained similar atomic structures in almost all cases. Consequently, for relaxing configurations prior to *ab initio* calculations, one could use any classical potential. However, for investigating stability, it is necessary to consider several kinds of potential.

## § 6. Conclusion

Using anisotropic elasticity theory, several semiempirical classical potentials and first-principles calculations, we have investigated the properties of the undissociated screw dislocation in silicon. Considering previous studies and the geometry of the silicon atomic structure, three possible structures have been selected and compared. We have shown that configuration A, where the dislocation core is located in the centre of one hexagon, in the shuffle set, is clearly more stable than the other two configurations. In a previous study by Koizumi *et al*. (2000), another configuration, with the dislocation located in the centre of one long hexagon edge, was favoured. From our calculations, it appears that this result is explained by the use of the SW potential, this configuration being less stable with other classical potentials or *ab initio* methods. We also investigated a third solution, with the dislocation in the glide set. Despite its high defect energy, this configuration presents the interesting feature of an $sp^2$ hybridization of the atoms forming the core. Obviously, such a structure is worth studying in a material favouring $sp^2$, such as diamond. We also characterized the spatial extension of the cores of each structure by determining the derivative of the disregistry. A possible continuation of this work includes the determination of the mobility of the undissociated screw dislocation in silicon. The study of other dislocation orientations, such as those recently observed at low temperatures (Rabier *et al*. 2000, 2001), would be another working direction.

## References

ABINIT, 2002, URL http://www.pcpm.ucl.ac.be/abinit.

Arias, T. A., and Joannopoulos, J. D., 1994, *Phys. Rev. Lett*., **73**, 680.

Bigger, J. R. K., McInnes, D. A., Sutton, A. P., Payne, M. C., Stich, I., King-Smith, R. D., Bird, D. M., and Clarke, L. J., 1992, *Phys. Rev. Lett*., **69**, 2224.

Blumenau, A. T., Heggie, M. I., Fall, C. J., Jones, R., and Frauenheim, T., 2002, *Phys. Rev*. B, **65**, 205 205.

Bulatov, V. V., Justo, J. F., Cai, W., Yip, S., Argon, A. S., Lenosky, T., de Koning, M., and Diaz de la Rubia, T., 2001, *Phil. Mag*. A, **81**, 1257.

Cai, W., Bulatov, V. V., Chang, J., Li, J., and Yip, S., 2001, *Phys. Rev. Lett*., **86**, 5727.

Duesbery, M. S., and Joos, B., 1996, *Phil. Mag*. A, **74**, 253.

Ewels, C. P., Wilson, N. T., Heggie, M. I., Jones, R., and Briddon, P. R., 2001, *J. Phys.: condens. Matter*, **13**, 8965.

George, A., and Michot, G., 1993, *Mater. Sci. Engng*, **A164**, 118.

Hirsch, P. B., Roberts, S. G., and Samuels, S., 1989, *Proc. R. Soc*. A, **421**, 25.

Hirth, J. P., and Lothe, J., 1982, *Theory of Dislocations* (New York: Wiley).

Hohenberg, P., and Kohn, W., 1964, *Phys. Rev*., **136**, B864.

Hornstra, J., 1958, *J. Phys. Chem. Solids*, **5**, 129.

Justo, J. F., Bazant, M. Z., Kaxiras, E., Bulatov, V. V., and Yip, S. 1998, *Phys. Rev*. B, **58**, 2539.

Kaxiras, E., and Duesbery, M. S., 1993, *Phys. Rev. Lett*., **70**, 3752.

Kohn, W., and Sham, L. J., 1965, *Phys. Rev*., **140**, A1133.

Koizumi, H., Kamimura, Y., and Suzuki, T., 2000, *Phil. Mag*. A, **80**, 609.

Lehto, N., and Öberg, S., 1998, *Phys. Rev. Lett*., **80**, 5568.

MIYATA, M., and FUJIWARA, T., 2001, *Phys. Rev.* B, **63**, 045 206.
MONKHORST, H. J., and PACK, J. D., 1976, *Phys. Rev.* B, **13**, 5188.
RABIER, J., CORDIER, P., TONDELLIER, T., DEMENET, J. L., and GAREM, H., 2000, *J. Phys.: condens. Matter*, **49**, 10 059.
RABIER, J., CORDIER, P., DEMENET, J. L., and GAREM, H., 2001, *Mater. Sci. Engng*, **A309–A310**, 74.
RAY, I. L. F., and COCKAYNE, D. J. H., 1971, *Proc. R. Soc.* A, **325**, 543.
SIMMONS, G., and WANG, H., 1971, *Single Crystal Elastic Constants and Calculated Aggregate Properties: A Handbook* (Cambridge, Massachusetts: MIT Press).
STILLINGER, F. H., and WEBER, T. A., 1985, *Phys. Rev.* B, **31**, 5262.
STROH, A. N., 1958, *Phil. Mag.*, **3**, 625; 1962, *J. math. Phys.*, **41**, 77.
SUZUKI, T., NISHISAKO, T., TARU, T., and YASUTOMI, T., 1998, *Phil. Mag. Lett.*, **77**, 173.
SUZUKI, T. YASUTOMI, T., TOKUOKA, T., and YONENAGA, I., 1999a, *Phys. Sat. sol.* (a), **171**, 47; 1999b, *Phil. Mag.* A, **79**, 2637.
TERSOFF, J., 1988, *Phys. Rev.* B, **38**, 9902.
TROUILLER, N., and MARTINS, J. L., 1991, *Phys. Rev.* B, **43**, 1993.